Monte Carlo Simulation Scheme for Dendrimers Satisfying Detailed Balance

E. J. Wallace,[†] D. M. A. Buzza,*[,†] and D. J. Read[‡]

Department of Physics & Astronomy and Polymer IRC, University of Leeds, Leeds LS2 9JT, U.K.; and Department of Applied Mathematics, University of Leeds, Leeds LS2 9JT, U.K.

Received March 7, 2001; Revised Manuscript Received June 25, 2001

ABSTRACT: A lattice Monte Carlo scheme for simulating dendrimers that is widely referenced in the literature is that of Mansfield and Klushin (*Macromolecules* **1993**, *26*, 4262). However, we show that this scheme does not obey a detailed balance and propose a modification to the original scheme that fixes this problem. To demonstrate the importance of detailed balance to the simulation results, we calculate the radius of gyration and structure factor for ideal dendrimers using our improved model and compare our results to Mansfield and Klushin's original scheme and exact analytical calculations. Excellent agreement is found between our model and the exact analytical calculations, while surprisingly large discrepancies are found between Manfield and Klushin's original scheme and the exact calculations. Our study highlights the importance of detailed balance generally to Monte Carlo simulations of dendrimers and the need to check previous results for nonideal dendrimers obtained from nondetailed balance schemes; we discuss the extension of our model to the nonideal dendrimer case.

1. Introduction

Dendrimers are highly branched molecules with highly controlled structures and a large number of terminal-groups. Their unique molecular topology gives rise to many striking static and dynamic properties and offer potential applications in areas as diverse as drug delivery, chemical catalysis, viscosity modification, etc.[1,2] A key to utilizing and harnessing many of the interesting properties of dendrimers lies in understanding their molecular configurations under different conditions of interest. An exciting development in the field is the recent emergence of direct scattering studies that probe the detailed internal stucture of dendrimers;[3−11] the correct interpretation of these experimental data however relies on having reliable theoretical models for dendrimers. Both of these factors serve as a strong driving force for seeking theoretically methods to model this class of novel materials.

Monte Carlo simulations, both on-lattice[12] and off-lattice,[13,14] represent a powerful theoretical tool in modeling equilibrium properties of dendrimers. The advantage of Monte Carlo simulations compared to other simulation techniques, e.g., molecular dynamics, is that one is allowed unphysical moves which can greatly speed up the equilibration process.[15] This can be a distinct advantage for the study of dendrimers where the intramolecular monomer concentration is high (especially for higher generations) so that the relaxation dynamics are very slow. In this paper, we shall focus on lattice Monte Carlo simulations of dendrimers. Lattice models have the advantage that the interaction energies between particles are particularly simple: short-range hard-core repulsions can be accounted for by imposing incompressibility—i.e., each lattice site can only be occupied by at most one particle—while longer range interactions (e.g., van der Waals' interactions) can be accounted for by nearest neighbor interactions. A lattice Monte Carlo scheme for simulating dendrimers that is widely referenced in the literature is that of Mansfield and Klushin[12] (hereafter referred to as the MK scheme). This scheme has the advantage that it is elegant and samples phase space efficiently. However, we show that it does not obey detailed balance and propose a modification to the original scheme that fixes this problem. Detailed balance is a necessary but not sufficient condition for a simulation to achieve thermal equilibrium.[15] To demonstrate the importance of detailed balance to the simulation results, we calculate the radius of gyration and structure factor for ideal dendrimers (where exact results can be obtained) using our improved model, the MK scheme, and exact analytical calculations. Excellent agreement is found between our model and the exact calculations, while surprisingly large discrepancies are found between the MK scheme and the exact calculations. Our study represents a step forward in the proper simulation of dendrimers and will hopefully help in the understanding of recent experimental scattering studies and more generally lead to a better utilization of the unique properties of dendrimers.

The rest of the paper is organized as follows. In section 2, we give details of our lattice Monte Carlo simulation together with a discussion of the detailed balance condition in the context of the simulation. The results of our simulations and the comparison to the MK scheme and exact calculations are presented in section 3, and section 4 contains our conclusions.

2. Details of Monte Carlo Simulation

Our Monte Carlo scheme follows closely that of the MK scheme.[12] However where we differ critically from their scheme is the way in which we calculate the acceptance criterion for trial moves of nonterminal spacers (see later in this section). Following the MK scheme, we consider a dendrimer laid out on a diamond lattice. The central core of the dendrimer is connected to three spacers. Each of these spacers is connected to two other spacers, and they in turn are connected to

[†] Department of Physics & Astronomy and Polymer IRC, University of Leeds.
[‡] Department of Applied Mathematics, University of Leeds.

10.1021/ma0104130 CCC: $20.00
Published on Web 08/30/2001

two other spacers etc. so that the number of spacers increases by a factor of 2 going from one generation to the next. The connectivity between spacers for the first few generations of dendrimers is illustrated in Figure.1. All spacers in the dendrimer consist of seven-step walks on the lattice. Note that we use the counting convention for the generation number g where a three-arm star is considered to be a $g = 0$ dendrimer.

We adopt the same coordinate system as in the MK scheme where valid steps on the diamond lattice consist of any of the following eight vectors:

$$a = (+1, +1, +1), \quad a' = -a$$

$$b = (-1, -1, +1), \quad b' = -b$$

$$c = (-1, +1, -1), \quad c' = -c$$

$$d = (+1, -1, -1), \quad d' = -d$$

Valid walks on the lattice are any sequences of the eight vectors satisfying the condition that primed and unprimed vectors must alternate in the walk. Note that we are working with the units of length where a lattice step has length $3^{1/2}$. To compare our simulation results to exact analytical results, we consider the case of ideal dendrimers (i.e., where all monomer−monomer interactions are absent) where exact analytical results can be obtained. We therefore allow back steps; this is in contrast to the original paper of Mansfield and Klushin where the simulation was performed on self-avoiding dendrimers and where back-steps are therefore disallowed. Since there are eight choices for the first step and four for subsequent steps, there are 32 768 possible seven-step spacer configurations. These configurations are divided into two parity classes of 16 384 configurations each, depending on whether the first step in the spacer is primed or unprimed. For a faithful representation of dendrimer configurations in the simulation, all spacers in the same generation are required to have the same parity, and because we are working with spacers that have an odd number of steps, the spacer parity is required to alternate from one generation to the next. To increase computational speed, all 32 768 spacer configurations are generated beforehand and then sorted and stored as a look-up table according to parity and end-to-end vector.

We recall that a Monte Carlo move consists of two stages. First we perform a trial move from state o to state n. We denote the probability for the trial move as $\alpha(o \rightarrow n)$. The next stage is to determine whether to accept this trial move. We denote the probability for accepting the trial move as $\mathrm{acc}(o \rightarrow n)$. The probability of the transition $o \rightarrow n$ is then given by $\pi(o \rightarrow n) = \alpha(o \rightarrow n) \times \mathrm{acc}(o \rightarrow n)$.

In our simulation, a Monte Carlo move begins with a random selection of a spacer in the dendrimer. Following the MK scheme, we perform two fundamental types of trial moves depending on whether the selected spacer belongs to the last generation (i.e., an "end spacer") or to a generation other than the last (i.e., an "internal spacer"). If the chosen spacer is an end spacer, an "end wiggle" is performed, while if an internal spacer is chosen, we perform an "internal" wiggle (see Figure 2).

An end wiggle is performed by replacing the configuration of the chosen spacer by one of the 16 384 possible configurations having the same parity. Since we are considering an ideal dendrimer and the new spacer configuration is always physical, the new configuration is always accepted.

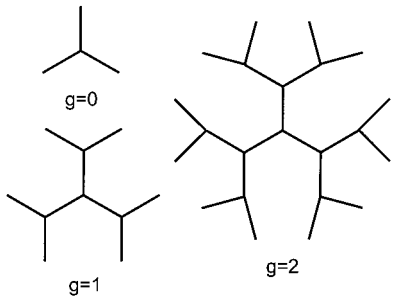

Figure 1. $g = 0$, 1, 2 dendrimers.

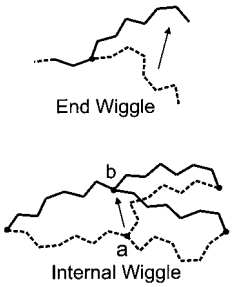

Figure 2. End wiggle and internal wiggle.

An internal wiggle involves the selected internal spacer and its two daughters. Together, these three form a three-legged "spider". In an internal wiggle, the three "feet" of the spider (i.e., the nodes where the legs of the spider terminate) are kept stationary, while the central node of the spider is displaced by one of the following 12 vectors, selected at random: $(\pm2, \pm2, 0)$, $(\pm2, 0, \pm2)$, $(0, \pm2, \pm2)$. The look-up table of spacer configurations is then scanned for spacer states having the correct parity and end-to-end vector in order to bridge the gaps between each foot of the spider and the new central node. A successful internal wiggle therefore leaves the three feet of the spider stationary while allowing all other parts of the spider to move (see Figure 2). If more than one spacer configuration can be found between any one foot and the central node, the new trial configuration is formed by selecting one of the possible spacer configurations to form the new spacer configurations between that foot and the central node. Therefore, for an internal wiggle, $\alpha(a \rightarrow b) = \alpha(b \rightarrow a) = {}^1/_{12}$, where a and b are the central node positions before and after an internal wiggle, respectively.

Where our simulation scheme differs subtlely but critically from that of the MK scheme is in the acceptance criterion for internal wiggles. In the MK scheme, provided that spacer configurations can be found to bridge the gap between each foot and the central node (i.e., the trial configuration for the three legged spider is physical), the internal wiggle is accepted with a probability which is Boltzmann weighted to the difference in energy between the new and old configuration; i.e.,

$$\mathrm{acc}(a \rightarrow b) = \min(1, \exp[-(E_{\mathrm{ib}} - E_{\mathrm{ia}})/k_{\mathrm{B}}T]) \quad (1)$$

where E_{ia} and E_{ib} are the energies of the specific microstates i_{a} and i_{b} having central node positions a and b, respectively. For ideal chains, this reduces to

$$\mathrm{acc}(a \rightarrow b) = 1 \quad (2)$$

Equation 1 satisfies the following "detailed balance" condition:

$$N(i_a) \times \alpha(a \rightarrow b) \times \mathrm{acc}(a \rightarrow b) = N(i_b) \times \alpha(b \rightarrow a) \times \mathrm{acc}(b \rightarrow a)$$

where $N(i_a) = \exp(-E_{ia}/k_BT)/Z$ and $N(i_b) = \exp(-E_{ib}/k_BT)/Z$ are the probabilities of the system being in the microstates i_a and i_b, respectively (Z is a normalization constant, i.e., the partition function). However, this does not actually satisfy detailed balance because in general there are many other microstates having central node positions a and b, each with different occupation probabilities. The correct detailed balance condition should be

$$N(a) \times \alpha(a \rightarrow b) \times \mathrm{acc}(a \rightarrow b) = N(b) \times \alpha(b \rightarrow a) \times \mathrm{acc}(b \rightarrow a) \quad (3)$$

where

$$N(a) = \sum_{i_a} N(i_a) = \frac{1}{Z}\sum_{i_a} \exp(-E_{i_a}/k_BT) \quad (4)$$

$$N(b) = \sum_{i_b} N(i_b) = \frac{1}{Z}\sum_{i_b} \exp(-E_{i_b}/k_BT)$$

are the probabilities that the system is in *any* microstate having node positions a and b, respectively. To satisfy detailed balance, we therefore use a modified acceptance criterion given by

$$\mathrm{acc}(a \rightarrow b) = \min\left(1, \frac{N(b)}{N(a)}\right) \quad (5)$$

For ideal chains, all microstates are equally likely to be occupied. The calculation of $N(a)$ and $N(b)$ therefore reduces to a problem of counting the number of microstates having node positions a and b, respectively, i.e.,

$$\frac{N(b)}{N(a)} = \frac{N_{1b} \times N_{2b} \times N_{3b}}{N_{1a} \times N_{2a} \times N_{3a}} \quad (6)$$

where N_{1a}, N_{2a}, N_{3a} and N_{1b}, N_{2b}, N_{3b} are the numbers of spacer configurations with the correct parity and end-to-end vector to bridge the gaps between the three feet of the spider and node positions a and b, respectively. Note that in our implementation of the computer program, the values of N_{1a}, N_{2a}, N_{3a} and N_{1b}, N_{2b}, N_{3b} are available at the outset from our look-up table.

Equation 5 has a simple interpretation in the case of ideal chains. Since all states have equal probability of occupation, ergodicity will favor branch point positions of the dendrimer which are associated with a greater number of microstates. Equation 5 reflects this bias. The absence of this bias in the MK scheme (see eq 2) leads to a nonequilibrium distribution of states where the system spends a disproportionately long time in statistically less likely branch point positions where the spacers connected to the branch points are too strongly stretched. In general, for both ideal and nonideal dendrimers, $N(b)/N(a)$ will be significantly different from $N(i_b)/N(i_a)$, so that the MK scheme deviates from the detailed balance. The violation of detailed balance leads to surprisingly large errors in the simulation results as we shall see in the next section.

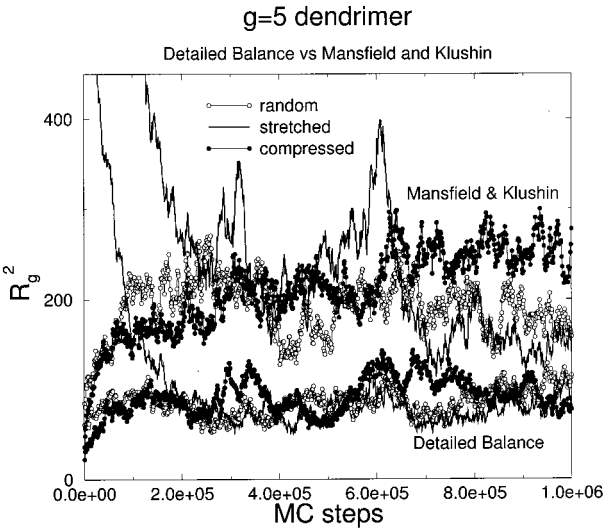

Figure 3. Relaxation of the radius of gyration for a $g = 5$ dendrimer starting from three different initial structures (random, stretched, and compressed). The top three curves are from the MK scheme while the bottom three curves are from the DB scheme.

Three different techniques were used to generate initial configurations for the Monte Carlo simulations. In the first technique, which produces what we call "random" initial structures, the initial state of all the spacers in the dendrimer are generated by random selection from the look-up table of spacer states. In the second technique, which produces what we call "stretched" states, the three spacers in $g = 0$ are selected randomly from all spacer states where the end-to-end vector modulus is greater than or equal to 7. The initial state of all spacers "descendant" from each of these three spacers is then generated by a random selection from all spacer states where the end-to-end vector modulus is greater than 7 and where the end-to-end vector belongs to the same quadrant as the "ancestor" spacer in $g = 0$. This produces a highly stretched initial structure. In the third technique, which produces what we call "compressed" initial states, the initial state of all the spacers in the dendrimer is generated by a random selection from all spacer states where the modulus of the end-to-end vector is equal to 1. This produes a highly compressed initial state. To ensure that we have reached true equilibrium before commencing data collection, we performed three parallel runs for each generation of dendrimer, starting from the three different initial structures outlined above. We define the point where the radius of gyration (R_g) from the three runs first converge to the same average value as the point where thermal equilibrium has been achieved. For example in Figure 3, we show the radius of gyration results for a $g = 5$ dendrimer. According to our criterion, thermal equilibrium had been achieved at about 2×10^5 and 3×10^5 Monte Carlo steps for the detailed balance and MK schemes, respectively. The number of Monte Carlo steps required for equlibration N_{eq} is reported in Table 1 for each dendrimer generation; note that since N_{eq} was found to be roughly the same for both detailed balance and MK schemes, only one value for N_{eq}, corresponding to the value for the detailed balance scheme, was reported for each g.

Table 1. Number of Monte Carlo Steps Required for Equlibration (N_{eq}) for Each Dendrimer Generation

g	N_{eq}
1	$<10^3$
2	2×10^3
3	2×10^4
4	5×10^4
5	2×10^5

To ensure good statistics for averaging, runs of 1000 $\times$ N_{eq} Monte Carlo steps were performed for each simulation. At intervals of N_{eq}/10steps, the radius of gyration squared R_g^2 was calculated, while at intervals of N_{eq} steps, the structure factor $S(q)$ was calculated. To ensure that system was truly in equilibrium before averaging, averaging was only performed on data collected from $10N_{eq}$ MC steps onward. This means that the averaging for R_g^2 was performed using about 10^4 data points while the averaging for $S(q)$ was performed using about 10^3 data points. R_g^2, $S(q)$ were calculated from

$$R_g^2 = \frac{1}{2N^2}\sum_{j=1}^{N}\sum_{k=1}^{N}(\mathbf{R}_j - \mathbf{R}_k)^2 \tag{7}$$

$$S(q) = \frac{1}{N^2}\sum_{j=1}^{N}\sum_{k=1}^{N}\frac{\sin(q|\mathbf{R}_j - \mathbf{R}_k|)}{q|\mathbf{R}_j - \mathbf{R}_k|} \tag{8}$$

where $\mathbf{R}_j$ is the position vector of the jth monomer, q is the magnitude of the scattering wave vector, and N is the total number of monomers in the dendrimer. In our calculation, we consider the monomers to be positioned on the lattice node at the end of each lattice step. The total number of monomers (including the monomer at the central core) is $N = 21(2^{g+1} - 1) + 1$.

3. Results and Discussion

As mentioned in the Introduction, detailed balance is a necessary but not sufficient condition for a simulation to achieve thermal equilibrium.[15] To demonstrate the importance of detailed balance to the simulation results for dendrimers, in this section we compare results on ideal dendrimers from Monte Carlo simulations using the modified acceptance criterion given by eqs 5 and 6, which we shall call the "detailed balance" (DB) scheme, and using the acceptance criterion given by eq 2, which we shall call the "Mansfield and Klushin" (MK) scheme. These results are compared to exact analytical calculations for ideal dendrimers, which are given explicitly in the Appendix.

In Table 2, we report results for R_g for different generation numbers and different initial configurations. We also report estimated errors in R_g. These are estimated from $\sigma/\sqrt{1000}$, where σ is the variance of the run; this is because each run consists of $1000N_{eq}$ MC steps, so the results can be viewed as being obtained from 1000 independent copies of the system. We note that within the same simulation scheme, results from different initial configurations are in excellent agreement with each other (within the error of the simulation) showing that we have obtained true steady-state values for R_g for both the DB and MK schemes. We also note that the error bars in the MK results are slightly greater than the DB scheme, reflecting the inherently larger fluctuations in the MK simulation (see Figure 3). This is due to the fact that all trial moves (except unphysical ones) are accepted in the MK scheme, while the acceptance rate is much lower for the DB scheme (typically acc($a \rightarrow b$) $\sim$ 0.2). However, the most striking feature about the results in Table 2 is the fact that the R_g values from the MK scheme are consistently 50% greater than that of the exact calculation for all values of g that we have studied. On the other hand, excellent agreement is found between the DB scheme and the exact calculations (within the error of the simulation). The large discrepancy between MK and the exact results is a direct consequence of detailed balance violation. As explained in the previous section, in the MK scheme, the system spends a disproportionate amount of time in branch point positions where the spacers connected to the branch point are too strongly stretched, which therefore leads to the radius of gyration being greater than the equilibrium value.

Table 2. Radius of Gyration for Different Generation Numbers and Initial Configurations (R = Random, S = Stretched, C = Compressed)

		R_g		
g	initial structure	detailed balance	Mansfield & Klushin	exact calculation
1	R	4.46 ± 0.02	6.11 ± 0.03	4.49
1	S	4.45 ± 0.02	6.10 ± 0.03	4.49
1	C	4.46 ± 0.02	6.10 ± 0.03	4.49
2	R	5.81 ± 0.03	8.52 ± 0.04	5.81
2	S	5.77 ± 0.03	8.47 ± 0.04	5.81
2	C	5.81 ± 0.03	8.45 ± 0.04	5.81
3	R	7.02 ± 0.03	10.52 ± 0.04	7.03
3	S	7.02 ± 0.03	10.57 ± 0.04	7.03
3	C	7.04 ± 0.03	10.60 ± 0.04	7.03
4	R	8.19 ± 0.03	12.49 ± 0.04	8.17
4	S	8.17 ± 0.03	12.48 ± 0.04	8.17
4	C	8.16 ± 0.03	12.43 ± 0.04	8.17
5	R	9.25 ± 0.03	14.30 ± 0.04	9.25
5	S	9.24 ± 0.03	14.33 ± 0.04	9.25
5	C	9.24 ± 0.03	14.31 ± 0.04	9.25

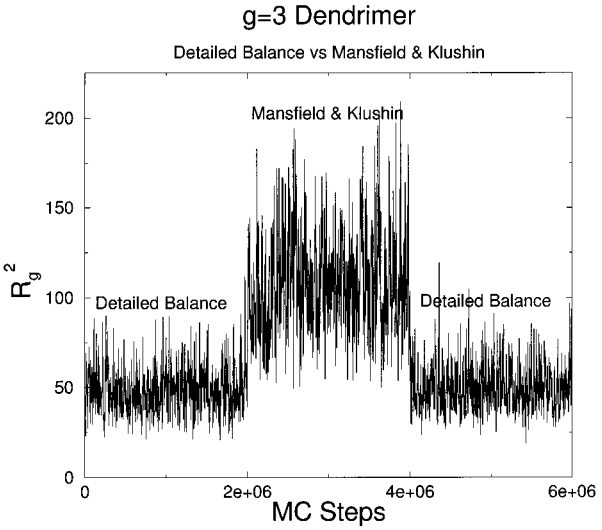

Figure 4. Change in radius of gyration for a $g = 3$ dendrimer when the acceptance probability given by eq 5 is switched off at 2×10^6 MC steps and switched on again at 4×10^6 MC steps.

The large difference in R_g generated by the two schemes is illustrated more dramatically in Figure 4. Here the simulation was carried out on a $g = 3$ dendrimer for 6 million MC steps. For the first 2 million steps, the detailed balance condition, i.e., eq 5, was applied; for the next 2 million steps, the detailed balance condition was switched off, i.e., eq 2 was applied; finally

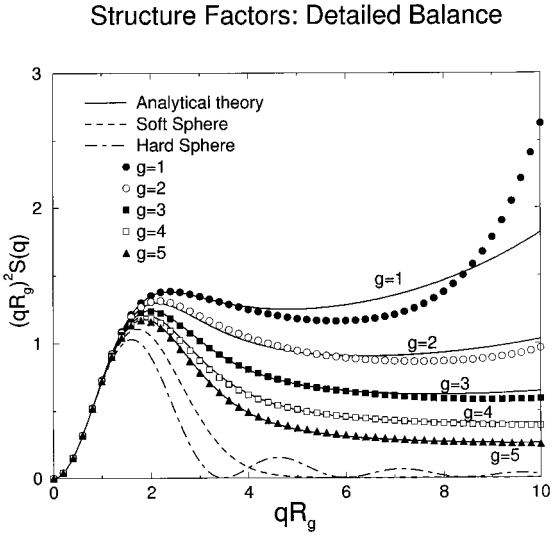

Figure 5. Kratky plot of scatterring structure factor comparing the DB scheme (data points) with the exact analytical calculation.

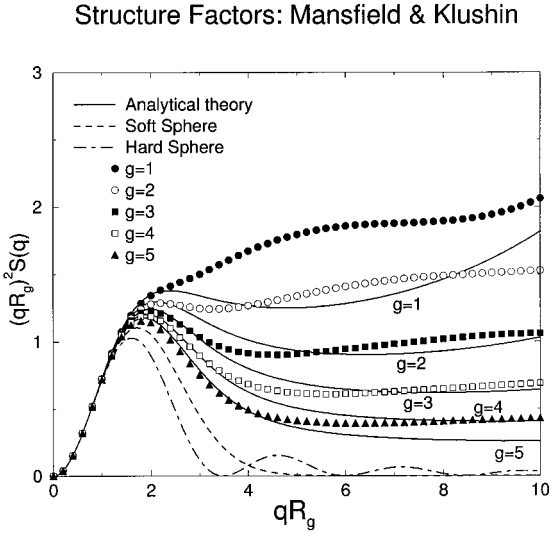

Figure 6. Kratky plot of scatterring structure factor comparing the MK scheme (data points) with the exact analytical calculation.

for the last 2 million steps, we switch the detailed balance condition back on. The large difference in the steady state R_g values is evidenced in Figure 4 by a sharp step up at 2 million MC steps and an equally sharp step down at 4 million MC steps. The sharpness of the steps shows the simulation scheme used samples phase space very efficiently so that the system is able to respond rapidly to changes in acceptance probabilities ($N_{eq} \approx 2 \times 10^4$ for $g = 3$ from Table 1). On the other hand, the complete reversibility in the change of the steady state R_g value shows that the steady-state values obtained from the simulation are true "equilibrium" values rather than metastable values due to the system being trapped in long-lived metastable states.

A more stringent test of the simulation is to compare the scattering structure factors $S(q)$ with the exact calculation. This is because $S(q)$contains information not only on the overall size of the molecule, but also of detailed monomer−monomer concentration correlations within the molecule. In Figure 5 we show a Kratky plot of $(qR_g)^2S(q)$ vs (qR_g) comparing the DB scheme to the exact analytical results for $g = 1-5$ dendrimers. Excellent agreement with the exact results is obtained for all the dendrimers at low q; discrepancies at high q and low g are due to differences in the microscopic details of the two approaches: the exact calculation assumed an off-lattice Gaussian chain model for the polymer chains while the simulation was performed for polymers on a lattice. We expect agreement between the two approaches to break down for $qb \gtrsim 1$, where b is the step length, i.e. $q \gtrsim 1/\sqrt{3} \approx 0.58$ in units of length where $b = \sqrt{3}$. Referring to Figure 5, we see that the breakdown in agreement occurs for $qR_g > 3 \Rightarrow q > 0.67$ for $g = 1$; $qR_g > 6 \Rightarrow q > 1.0$ for $g = 2$; $qR_g > 8 \Rightarrow q > 1.1$ for $g = 3$. For $g = 4$, 5, no appreciable discrepancy occurred within the plotted range of qR_g values. In other words the detailed balance scheme agrees with analytical theory in the q range where one would reasonably expect agreement. In Figure 6 we show the analogous Kratky plot comparing the MK scheme to the exact analytical calculation. We note that even after scaling the q axis by the $R_g$value appropriate to the MK scheme, the nondetailed balance scheme still fails to agree either quantitatively or even qualitatively with the exact results. This conclusively demonstrates the importance of the detailed balance condition to correctly simulate dendrimer properties, not only the overall size, but also the detailed monomer concentration correlations within the molecule.

While the current study has mainly focused on ideal dendrimers, our study highlights the importance of detailed balance generally to the Monte Carlo simulation of dendrimers. It is therefore imperative that previous results for nonideal dendrimers obtained from nondetailed balance schemes are checked again using modified Monte Carlo schemes which obey detailed balance. In principle, we could use our current scheme to do this, since eqs 4, 5 are also applicable to nonideal dendrimers. However a quick estimate of the number of states that would have to be summed over in eq 4 to calculate $N(a)$ and $N(b)$ for each Monte Carlo step will show such a computational scheme would very quickly become unfeasible, even for the fastest computers currently available. An alternative Monte Carlo simulation scheme therefore needs to be found, and we hope to discuss this in a future publication.

In Figures 5 and 6, we have also plotted $S(q)$ for a hard sphere and a soft sphere for comparison with our simulation data. For the hard sphere, $S(q) = [(3/X^3)(\sin X - X \cos X)]^2$, where $X = \sqrt{5/3}\, qR_g$ and $R_g^2 = {}^3/_5 r^2$, where r is the radius of the sphere. The soft sphere structure factor is given by $S(q) = \exp(-{}^1/_3 q^2 R_g^2)$ which represents the Guinier approximation for globular structures.[16] Not surprisingly, the simulation data in Figures 5 and 6 do not show any of the higher harmonics exhibited for hard spheres. This is because we have not put in hard core interactions between monomers in our simulation so that there is no sharp boundary in the monomer concentration profile to give rise to these harmonics. Interestingly, however, the simulated structure factors appear to approach the soft sphere $S(q)$ as we go to higher generations. This indicates that ideal dendrimers have a very diffuse monomer concentration profile, approaching that of a soft globular structure.

4. Conclusions and Future Work

A lattice Monte Carlo scheme for simulating dendrimers that is widely referenced in the literature is that

of Mansfield and Klushin. Although the scheme is elegant and samples phase space efficiently, we show that it does not obey detailed balance and propose a modification to the original scheme that fixes this problem. To demonstrate the importance of detailed balance to the simulation results, we calculated the radius of gyration R_g and structure factor $S(q)$ for ideal dendrimers (where exact analytical results can be obtained) and compared our improved model to the MK scheme and exact analytical calculations. We found excellent agreement between our model and the exact analytical calculations but surprisingly large discrepancies between the MK scheme and the exact calculations. This is true both of R_g and $S(q)$. While the current study has mainly focused on ideal dendrimers, our study highlights the importance of detailed balance generally to the Monte Carlo simulation of dendrimers. It is therefore imperative that previous results for nonideal dendrimers obtained from nondetailed balance schemes are checked again using modified Monte Carlo schemes which obey detailed balance. We propose to do this in a future publication using a Monte Carlo scheme that incorporates monomer−monomer interactions.

Acknowledgment. The authors gratefully acknowledge help from Dave Adolf on computational aspects of the paper.

Appendix A. Exact Analytical Method for Calculating Ideal Dendrimer Structure Factors

The structure factor of ideal dendrimers has been calculated previously by Burchard et al.[16] and Hammouda;[17] however, these derivations are rather complicated. In this appendix, we present an alternative derivation which is more compact and straightforward using the formalism developed by Read for calculating polymer structure factors.[18] We shall give a brief outline of the calculation here; for details the reader is referred to ref 18. The starting point for our calculation is the expression for the structure factor given by

$$S(q) = \frac{1}{N^2}\sum_{j=1}^{N}\sum_{k=1}^{N}\langle \exp[i\mathbf{q}\cdot(\mathbf{R}_j - \mathbf{R}_k)]\rangle \qquad (9)$$

where $\mathbf{R}_j$ is the position of the jth monomer. Note that eq 8 is the same as the above expression except for the fact that in eq 8 there is no ensemble average $\langle\cdots\rangle$, but an orientational average over $\mathbf{q}$ has been performed. Read has shown that the summation over monomer pairs in eq 9 can always be rewritten as a summation over "structural unit" pairs; for the dendrimer, we choose our structural units to be dendritic branches of generation g (see Figure 7). Denoting J_g and H_g as the "self-term" and "co-term", respectively, of a generation g dendritic branch, the structure factor of the g generation dendrimer is given by

$$S_g(q) = n_b J_g + n_b(n_b - 1)H_g^2 + 1 + 2n_b H_g \qquad (10)$$

where n_b is the number of dendritic branches connected to the core monomer ($n_b = 3$ in our case). The first term in eq 10 accounts for correlations between monomer pairs in the same dendritic branch; the second term in eq 10 accounts for correlations between monomer pairs in different dendritic branches; the last two terms are, respectively, the self-correlation of the core monomer and the correlation between the core monomer and all other monomers in the dendrimer. In an exactly analogous way, J_g and H_g can be expressed in terms of self- and co-terms of dendritic branches of lower generation (see Figure 7), i.e.,

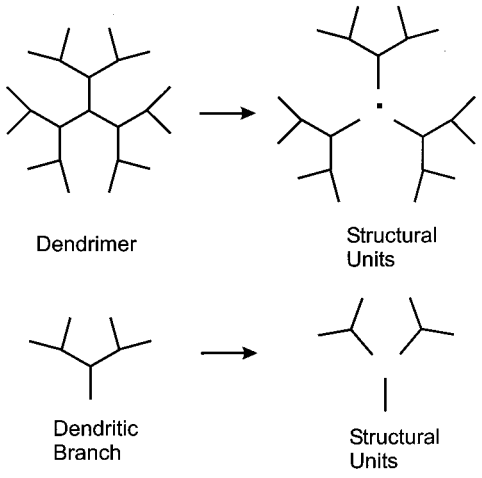

Figure 7. Structural units used to calculate the structure factor of a $g = 2$ dendrimer and dendritic branch.

$$H_g = H_0 + 2G_0 H_{g-1} \qquad (11)$$

$$J_g = J_0 + 2J_{g-1} + 4H_0 H_{g-1} + 2H_{g-1}^2 \qquad (12)$$

where J_{g-1}, H_{g-1} are the self-and co-terms respectively of dendritic branch of generation $g - 1$ and J_0, H_0, and G_0 are, respectively, the self-term, co-term, and "propagator" of a spacer (i.e., a generation 0 dendritic branch). Referring to Figure 7, the first and second term in eq 11 respectively account for contributions to H_g from monomers in the spacer and monomers in the $g - 1$ dendritic branches. Again referring to Figure 7, the first and second term in eq 12 respectively account for contributions to J_g from monomer pairs in the spacer and monomer pairs in the same $g - 1$ dendritic branch; the third term in eq 12 accounts for contributions to J_g from monomer pairs where one monomer is in the spacer and the other is in one of the $g - 1$ branches; the fourth term in eq 12 accounts for contributions to J_g from monomer pairs where the two monomers are in different $g - 1$ dendritic branches. Provided we know J_0, H_0, and G_0, therefore, S_g can be built up iteratively to arbitrary g using eqs 10−12. Calculating the structure factor for an ideal dendrimer therefore reduces to the problem of calculating J_0, H_0, and G_0.

For a spacer of n monomers, the quantities J_0, H_0, and G_0 are defined as

$$G_0 = \langle \exp[i\mathbf{q}\cdot(\mathbf{R}_n - \boldsymbol{R}_0)]\rangle$$

$$H_0 = \sum_{j=1}^{n}\langle \exp[i\mathbf{q}\cdot(\mathbf{R}_j - \boldsymbol{R}_0)]\rangle$$

$$J_0 = \sum_{j=1}^{n}\sum_{k=1}^{n}\langle \exp[i\mathbf{q}\cdot(\mathbf{R}_j - \mathbf{R}_k)]\rangle$$

where $\mathbf{R}_0$ is the position of the monomer to which the spacer is connected adjacent to monomer 1. Assuming a Gaussian chain model for the spacer, the above quantities can be easily calculated, and the result is

$$G_0 = \exp[-nQ_0^2] \tag{13}$$

$$H_0 = \sum_{j=1}^{n} \exp[-jQ_0^2] = \frac{1 - \exp[-nQ_0^2]}{\exp[Q_0^2] - 1} \tag{14}$$

$$J_0 = \sum_{j=1}^{n}\sum_{k=1}^{n} \exp[-|j-k|Q_0^2] = n + 2\frac{n(1 - \exp[-Q_0^2]) + \exp[-nQ_0^2] - 1}{(1 - \exp[-Q_0^2])(\exp[Q_0^2] - 1)} \tag{15}$$

where $Q_0^2 \equiv q^2b^2/6$. Analytical expressions for the radius of gyration R_g can be readily obtained from the following series expansion in q of $S_g(q)$:

$$S_g(q) = (1 - {}^1/_3 q^2 R_g^2 + ...) \tag{16}$$

However the resultant expressions for R_g are rather tedious and are therefore not reproduced here. Note that while the behavior of $S_g(q)$for $qb \gtrsim 1$ depends on the microscopic details of the model used (e.g., off-lattice Gaussian chain model, diamond lattice model, etc.), the results for R_g are more robust and are independent of the fine scale structure of the model so long as the same step length b is used. We therefore expect the R_g values calculated here from the Gaussian chain model to also hold exactly for our lattice Monte Carlo simulations.

References and Notes

(1) Voit, B. I. *Acta Polym.* **1995**, *46*, 87.
(2) Bosman, A. W.; Janssen, H. M.; Meijer, E. W. *Chem. Rev.* **1999**, *99*, 1665.
(3) Prosa, T. J.; Bauer, B. J.; Amis, E. J.; Tomalia, D. A.; Scherrenberg, R. *J. Polym. Sci., Part B: Polym. Phys.* **1997**, *35*, 2913−2924.
(4) Scherrenberg, R.; Coussens, B.; van Vliet, P.; Edouard, G.; Brackman, J.; de Brabander, E.; Mortensen, K. *Macromolecules* **1998**, *31*, 456−461.
(5) Potschke, D.; Ballauff, M.; Lindner, P.; Fischer, M.; Vogtle, F. *Macromolecules* **1999**, *32*, 4079−4087.
(6) Topp, A.; Bauer, B. J.; Tomalia, D. A.; Amis, E. J. *Macromolecules* **1999**, *32*, 7232−7237.
(7) Topp, A.; Bauer, B. J.; Klimash, J. W.; Spindler, R.; Tomalia, D. A.; Amis, E. J. *Macromolecules* **1999**, *32*, 7226−7231.
(8) Potschke, D.; Ballauff, M.; Lindner, P.; Fischer, M.; Vogtle, F. *Macromol. Chem. Phys.* **2000**, *201*, 330−339.
(9) Evmenenko, G.; Bauer, B. J.; Mischenko, N.; Forier, B.; Dehaen, W.; Kleppinger, R.; Amis, E. J.; Reynaers, H. *Physica B* **2000**, *276*, 349−350.
(10) Potschke, D.; Ballauff, M.; Lindner, P.; Fischer, M.; Vogtle, F. *J. Appl. Crystallogr.* **2000**, *33*, 605−608.
(11) Evmenenko, G.; Bauer, B. J.; Kleppinger, R.; Forier, B.; Dehaen, W.; Amis, E. J.; Mischenko, N.; Reynaers, H. *Macromol. Chem. Phys.* **2001**, *202*, 891−899.
(12) Mansfield, M. L.; Klushin, L. I. *Macromolecules* **1993**, *26*, 4262−4268.
(13) Chen, Z. Y.; Cui, S.-M. *Macromolecules* **1996**, *29*, 7943.
(14) Carl, W. *J. Chem. Soc., Faraday Trans.* **1996**, *92*, 4151.
(15) Frenkel, D.; Smit, B. *Understanding Molecular Simulation*; Academic Press: San Diego, CA, 1996.
(16) Burchard, W.; Kajiwara, K.; Nerger, D. *J. Polym. Sci., Phys. Ed.* **1982**, *20*, 157.
(17) Hammouda, B. *J. Polym. Sci., Part B* **1992**, *30*, 1387.
(18) Read, D. J. *Macromolecules* **1998**, *31*, 899.

MA0104130